

Measurement and Modeling of Nonlinear Power Law Media

Xuan Feng
College of Geo-Exploration:
Science and Technology
Jilin University
Changchun, China
fengxuan@jlu.edu.cn

Thomas Szabo
Biomedical Engineering
Boston University
Boston, USA
tlszabo@bu.edu

Stephen Brown
Earth Resources Laboratory
Massachusetts Institute of
Technology
Cambridge, USA
sbrown@mit.edu

Michael Fehler
Earth Resources Laboratory
Massachusetts Institute of
Technology
Cambridge, USA
fehler@mit.edu

Dan Burns
Earth Resources Laboratory
Massachusetts Institute of
Technology
Cambridge, USA
burns@mit.edu

Abstract— Traditional measurements of nonlinear and viscoelastic materials can be complicated by effects of frequency power law absorption and dispersion which affect harmonic generation and propagation. New combined measurement and modeling approaches are needed that account for both effects. The nonlinear interaction of two co-propagating ultrasound longitudinal waves are used to characterize induced viscoelastic changes occurring in material microstructure. A strong longitudinal wave pump affects the viscoelastic properties of the sample with dynamically applied strain and a weaker longitudinal wave probe senses induced changes. We developed a model which includes both nonlinearity and an estimation of viscoelastic characteristics to extract the second and third order nonlinear coefficients directly from the time domain data. Two samples, Lucite and Crab Orchard sandstone, have comparable viscoelastic properties but vastly different nonlinear characteristics. Additional signal processing was needed to extract parameters from the Lucite sample. Measurements for the Crab Orchard sandstone nonlinear coefficients were $\beta = -180$, and $\delta = -0.42 \times 10^{-9}$, and for Lucite, they were $\beta = -3.20$, and $\delta = 1.05 \times 10^{-6}$. Our method can describe and quantify both the nonlinear and viscoelastic properties of materials consistently; however for materials with lower α , improved instrumentation and processing are needed.

Keywords— *hysteresis, nonlinearity, viscoelasticity, strain, ultrasound*

I. INTRODUCTION

Traditional measurements of nonlinear and viscoelastic materials can be complicated by effects of frequency power law absorption and dispersion which affect harmonic generation and propagation. New combined measurement and modeling approaches are needed that account for both effects. Our time-domain approach shows that in order to accurately determine higher order nonlinear coefficients of highly viscoelastic materials such as rocks, frequency power law

absorption and dispersion must be included. The nonlinear interaction of two co-propagating ultrasound longitudinal waves are used to characterize induced viscoelastic changes occurring in material microstructure as explained in section II. A strong longitudinal wave pump affects the viscoelastic properties of the sample with dynamically applied strain and a weaker longitudinal wave probe senses induced changes. The highly nonlinear [1] elastic response of rocks has been shown to be caused by the rock's microstructure [2]. Methods to measure the nonlinear response of a rock may help us to better characterize its microstructure and to identify differences among rocks.

Many viscoelastic materials have an absorption characteristic that obeys a frequency power law [3,4],

$$\alpha = \alpha_0 |f|^y. \quad (1)$$

in which α_0 is an absorption coefficient in nepers/cm-MHz^y. Causality requires that a phase velocity dispersion accompany the absorption. In this study we compare two viscoelastic nonlinear materials which have comparable viscoelastic properties but vastly different nonlinear properties, Lucite and Crab Orchard sandstone. The material transfer functions of these two materials are plotted in Fig. 1. The top curves display absorption and the bottom curves indicate dispersion which is $2\pi f/c(2\pi f)$ where c is dispersive phase velocity [4].

The Fourier transform of the material transfer function is the material impulse response function (mirf) which is shown for both materials in Fig. 2. This mirf compactly encodes the absorption and dispersion information into an equivalent time waveform. For our modeling purposes we approximate this mirf by a symmetric exponential $\exp(-\gamma|t|)$ centered at the peak of the mirf and fit to the e^{-1} points of the mirf.

In order to study the nonlinear properties of these materials we use a nonlinear version of Hooke's law as a power series expansion [6, 7],

$$\sigma = E\varepsilon + \beta E\varepsilon^2 + \delta E\varepsilon^3 + O(\varepsilon^4), \quad (2)$$

where E is elastic modulus and terms β and δ are the quadratic and cubic nonlinear elastic coefficients, respectively up to the third order in strain. The nonlinear elastic modulus M is defined as follows:

$$M = E + \beta E\varepsilon + \delta E\varepsilon^2. \quad (3)$$

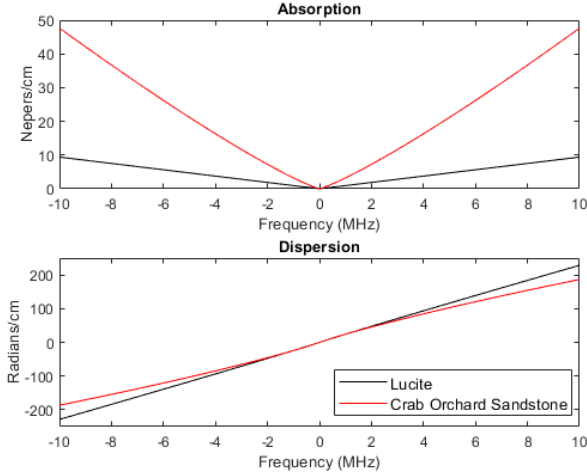


Figure 1. Material transfer functions for Lucite and crab orchard sandstone as a function of frequency

The normalized change in the elastic modulus with strain is

$$\Delta M/E = (M-E)/E = \beta\varepsilon + \delta\varepsilon^2. \quad (4)$$

However, we found from our experiments on viscoelastic materials that an additional term C must be included. Therefore, in order to fit the data, previous workers [8-11] using resonant steady state setups included a constant C :

$$\Delta M/E = C + \beta\varepsilon + \delta\varepsilon^2. \quad (5)$$

Because we use broadband time-varying waveforms of an arbitrary shape, we have extended this model to freely propagating, general time-varying strain (ε) waveforms by making the constant C dependent on the loading waveform time history as well as the maximum pump strain level. In addition, our experiments, which load a slowly time-varying strain field into rocks, show that C also empirically describes an observed offset of the modulus variation that is due to

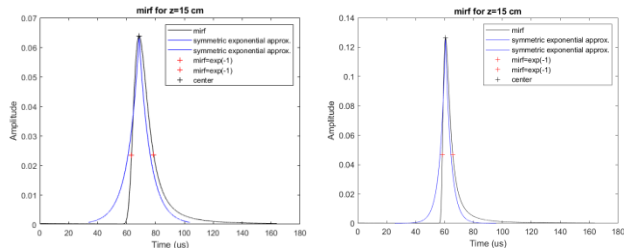


Figure 2 Material impulse response functions for crab orchard sandstone (left) and Lucite (right) as functions of time. Also shown are approximations as $\exp(-\gamma/|t|)$ functions with $\gamma=0.13$ for crab orchard sandstone and $\gamma = 0.23$ for Lucite with the $+$ $1/e$ points

nonlinear material conditioning [10-12]. In our model, C is a convolution of Eq. 4 and an approximation of a time domain viscoelastic response [4], $\exp(-\gamma/|t|)$ where γ is a viscoelastic parameter. If τ is a triggered offset delay in our experiments, the signal we measure [6] is

$$C(\tau) = e^{-\gamma/|\tau|} * [\beta\varepsilon(\tau) + \delta\varepsilon^2(\tau)]. \quad (6)$$

II. METHODS

A. Experimental Arrangement

For our present study, we use co-propagating longitudinal acoustic waves to load a strain field to measure the nonlinear characteristics of rock. As shown in Fig. 3, a low amplitude high-frequency (HF) longitudinal wave (the probe) travels from transmitter T1 to receiver R1. This signal is then compared to the probe signals under the influence of a high-amplitude low-frequency (LF) longitudinal wave (the pump), T2, that loads a temporally varying strain field in the rock. Probe signals are used to detect the elastic modulus variation induced by the loaded strain. This dynamic strain field offers a way to study the evolution of the elastic modulus variation between different strain cycles of the pump waveform directly in the time domain.

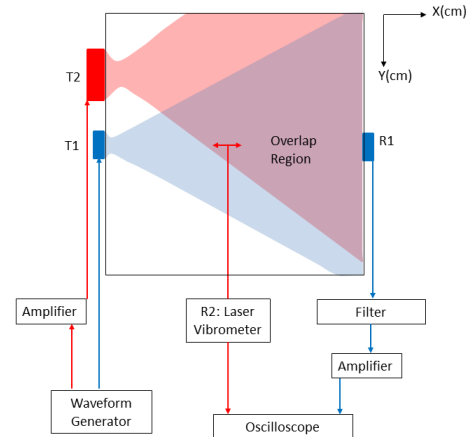


Figure 3. Co-propagating longitudinal wave experimental setup diagram. T1-R1: through transmission low energy high frequency probe pair; T2 is a high energy low frequency transmitting pump transducer. R2 is the laser vibrometer

Our setup depicted by Fig. 3 includes a pair of 1MHz HF (T1 and R1) 25 mm diameter compressional ultrasound transducers mounted on opposite sides of a sample (15 x 15 x 5 cm) to generate and receive 620 kHz probe signals, respectively. The pump is a high amplitude compressional source that loads a relatively high strain at 74 kHz into the sample through a 39 mm 0.1MHz LF (T2) transducer. The probe is a low amplitude signal that is used to measure small differences in arrival time that are induced by the large strains imposed by the pump transducer. As shown in Fig. 3, the pump beam (red) overlaps the probe beam (blue). Waves generated by the pump and probe propagate at the same

velocity. We selected the frequencies to maximize the amplitudes of the signals that were coupled into the sample while maintaining a large difference in frequencies between the pump and probe to facilitate measurements. Each applied pump voltage level corresponded to a maximum strain amplitude in the sample. A 3-component laser vibrometer (R2) measures the particle vibration velocity, $v(t)$, of the pump signal in the overlap region, which is used to estimate the strain, $\epsilon(t)$, induced into the sample. We record probe waveforms under two conditions at R1. One is the time-of-flight probe signal recorded when the pump signal is present (TOF). The other one is the time of the probe signal in the absence of the pump signal (TOF₀). Comparing TOF and TOF₀, we obtain a measure of the TOF delay, ΔTOF , which is used to calculate the elastic modulus variation induced by the pump.

B. Maintaining Elastic Modulus Estimation

In our experimental setup, the triggers of the probe signal were sequentially delayed over a range of 0-43 μs with 1 μs increments relative to the pump trigger to allow the probe signal to interact with various segments of the positive and negative strains induced by the pump signal. For each probe trigger time delay, we measured probe signals with and without the presence of the pump signal. A time-of-flight, TOF, delay, ΔTOF , between the two types of probe signals (with and without the pump on) depends on the trigger delay time. ΔTOF can be measured by a cross-correlation algorithm. The elastic modulus variation, $\Delta\text{M/E}$, is estimated as being proportional to the ΔTOF induced by the application of the pump divided by the original non-pump TOF₀ [13]:

$$\Delta\text{M/E} = -2 \Delta\text{TOF}/\text{TOF}_0 \quad (7)$$

where TOF₀ is the TOF of the probe in the absence of the pump signal (about 52.3 μs).

To obtain the strain as a function of time, the x-axis component of the particle velocity measured by the laser vibrometer, $v_x(t)$, is used to calculate the estimated strain at position (x,y) along the beam axis between the probe transducers:

$$\epsilon(t) = -v_x(t)/v_p, \quad (8)$$

where v_p is the longitudinal wave velocity in the rock sample (about 2870 m/s). For our viscoelastic model we fit Eq. 5 to the data given by Eq. 7 [6] by using $\epsilon(t)$ as an intermediate variable to determine the unknown parameters of delay, γ , β and δ .

III. RESULTS

A. Comparison of elastic modulus variation with time-varying strain for two materials

In top half of Fig.4, we present our measurements of strain in the Lucite and Crab Orchard samples according to Eq. 8. Despite the comparable strain levels in each material, the nonlinear responses are vastly different as given by the curves in the bottom half of the figure. The Lucite response is barely perceptible on this scale and is buried in noise.

In order to improve the weak Lucite signals, we examined the spectrum of the strain waves. Based on these spectra we

applied a Gaussian filter from 4 to 15Hz to the data. We used a model previously described [6] in the filtered results for the Crab Orchard Sandstone (Fig.5) at a maximum strain in Lucite of 4.88×10^{-7} . This model based on Eq.'s (5) and (6) is equated to the data of Eq. (7). A minimization method described in [6] was used to extract nonlinear and viscoelastic parameters, delay, γ , β and δ .

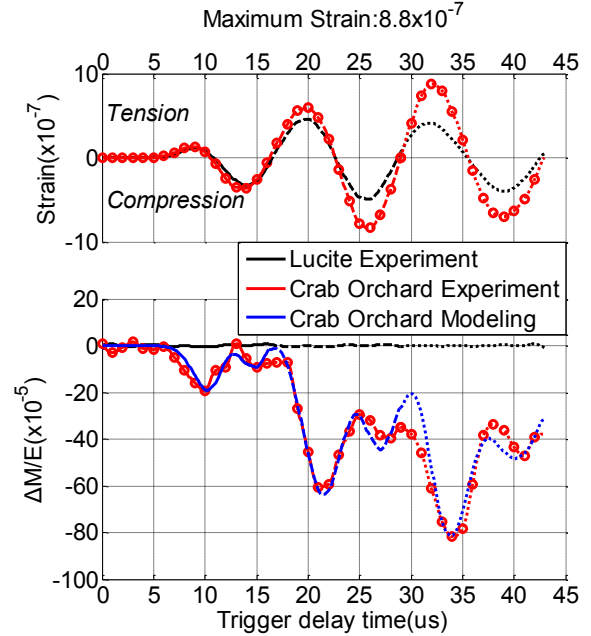


Figure 4. The top figure shows strain and the bottom figure indicates the elastic modulus variation, $\Delta\text{M/E}$, derived from probe signals both as functions of the trigger delay time. Black and red lines indicate results for the Lucite and Crab Orchard sandstone samples, respectively. The dotted blue curve indicates the modeling.

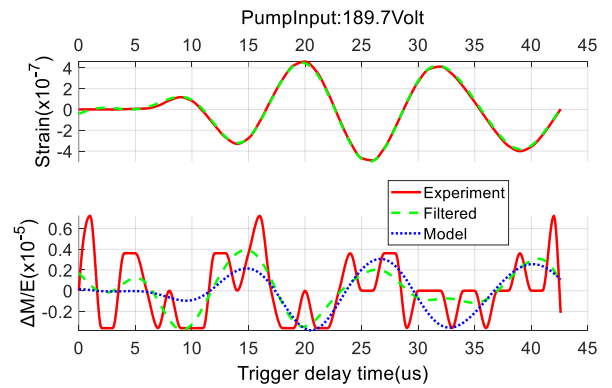


Figure 5. Top: red- Strain curve with a maximum strain of 4.88×10^{-7} . Dashed green- strain curve with strain frequency filter. Bottom : red- raw data, green-dashed- data filtered strain filter and blue- viscoelastic nonlinear model based on filtered data for the Lucite sample.

When the same process was applied to the data for Lucite in Fig. 5, the filtering of the noisy data improved the

modeling as can be seen in Fig. 5. Extracted parameters for both materials are compiled in Table 1.

B. Noise Study

In order to examine the effect of noise on the determination of parameters, random Gaussian noise with an r.m.s amplitude equal to the maximum amplitude of the baseline curve was added to the model baseline from Fig. 5. Fifty iterations of random noise with a signal to noise ratio of one were run to obtain a mean and standard deviation for each parameter. Results are in Table 2. A typical run is shown in Fig. 6.

Table 2.

params	γ_{nmean}	γ_{nstdev}	β_{nmean}	β_{nstdev}	δ_{nmean}	δ_{nstdev}
Lucite	.5376	.1941	-3.49	.5466	1.2e-6	8.84e-5

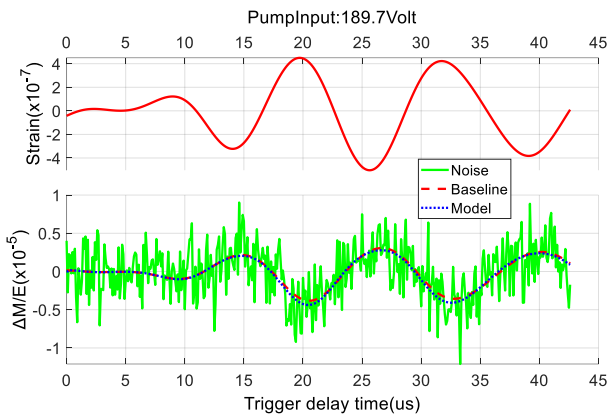


Figure 6. Top: Strain curve with a maximum of 4.88×10^{-7} . Bottom: green-baseline with random noise added, red-dashed-baseline, blue-dots-corresponding nonlinear model for the Lucite sample.

IV. DISCUSSION

The instrumentation (Fig.3) was designed for rocks with high nonlinear coefficients. In order to understand the effects of noise on low amplitude signals, we added random noise to a baseline to study the levels of uncertainty in determining parameters. From Table 2, for example, the standard deviation for β is 0.5466 corresponding to a per cent ratio of the standard deviation with noise to the mean value with noise of 15.66 %. Filtering reduced the ratio of the r.m.s error of the difference between the model and data to the model mean for $\Delta M/E$ from 1.15 to 0.562. What is measured in Fig.5 and Eq. 7 is time delay and the noise is most likely due to time quantization errors which do not resemble additive random noise. Our value for β are comparable to those reported elsewhere [8,15]. The model values for γ for Lucite are in the same ratio to the linear values for the Crab Orchard Sandstone (Fig.2). The delay parameter Δt , associated with a short term viscoelastic memory effect[6], was 0.9 for the sandstone and zero for Lucite.

V. CONCLUSION

Our experimental setup works well to characterize sedimentary rocks which have both viscoelasticity and large nonlinear coefficients due to pore space microstructure such as populations of microcracks. However, for weakly nonlinear materials such as Lucite, additional filtering was needed to obtain reasonable values. With improved instrumentation, we believe our proposed methodology can characterize a wider range of nonlinear, viscoelastic materials.

VI. ACKNOWLEDGEMENT

This work was supported by the National Key Research and Development Program of China (2016YFC0600505), by Weatherford through the MIT Energy Initiative, and by Chinese Geologic Survey project (DD20160207).

VII. REFERENCES

- [1] P. A. Johnson, B. Zinsner, and P. N. J. Rasolofosaon, Resonance and elastic nonlinear phenomena in rock, *J Geophys Res-Sol Ea*, 101(B5), 11553-11564, 1996.
- [2] T. W. Darling, J. A. TenCate, D. W. Brown, B. Clausen, and S. C. Vogel, "Neutron diffraction study of the contribution of grain contacts to nonlinear stress-strain behavior," *Geophys Res Lett*, 31(16), 2004.
- [3] Szabo vsco time T. L. Szabo and J. Wu, "A model for longitudinal and shear wave propagation in viscoelastic media," *J. Acoust. Soc. Am.*, 107(5), May 2000, pp2437-2446.
- [4] Szabo, T. L., Diagnostic ultrasound imaging : inside out, Second edition. ed., Elsevier, Amsterdam ; Boston, 2014, pp 93-99.
- [5] T. Gallot, A. Malcolm, T. Szabo, S. Brown, D. Burns, M. Fehler, "Characterizing the nonlinear interaction of S- and P-waves in a rock sample," *J Appl Phys*, 117(3) 034902, 2015.
- [6] X. Feng, M. Fehler, S. Brown, T. L. Szabo, and D. Burns, "Short period nonlinear viscoelastic memory of rocks revealed by co-propagating longitudinal acoustic waves", *Journal of Geophysical Research- Solid Earth* 123, 2018, <https://doi.org/10.1029/2017JB015012>
- [7] X. Feng, M. Fehler, S. Brown, D. Burns, T. Szabo, "Through Transmission Measurement of the Nonlinear Viscoelastic Memory of Rocks by Co-Propagating Longitudinal Ultrasonic Pulses," 2017 IEEE Ultrasonics Symposium Proceedings, Washington, D.C., 2017.
- [8] G. Renaud, P.-Y Le Bas, and P. A. Johnson, "Revealing highly complex elastic nonlinear (anelastic) behavior of Earth materials applying a new probe: Dynamic acoustoelastic testing," *Journal of Geophysical Research: Solid Earth*, B06202, 1-17, 2012.
- [9] J. A TenCate, K. E. A. Van den Abeele, T. J. Shankland, and P. A. Johnson, "Laboratory study of linear and nonlinear elastic pulse propagation in sandstone," *J Acoust Soc Am*, 100(3), 1383-1391, 1996.
- [10] K. E.A. Van den Abeele. "Elastic pulsed wave propagation in media with second- or higher-order nonlinearity .1. Theoretical framework." *J. Acoust Soc Am*, 99(6):3334- 3345, 1996.
- [11] G. Renaud, P. Y. Le Bas, and P. A. Johnson, "Revealing highly complex elastic nonlinear (anelastic) behavior of Earth materials applying a new probe: Dynamic acoustoelastic testing," *J Geophys Res-Sol Ea*, 117, 2012.
- [12] G. Renaud, J. Riviere, S. Hauptert, and P. Laugier. "Anisotropy of dynamic acoustoelasticity in limestone, in uence of conditioning, and comparison with nonlinear resonance spectroscopy.," 133(6):3706-3718, 2013.
- [13] R. A. Guyer, and P. A. Johnson, *Nonlinear mesoscopic elasticity : the complex behaviour of granular media including rocks and soil*, Wiley-VCH, Weinheim, 2009, xiii, p395.
- [14] J. Riviere, P. Shokouhi, R. A. Guyer, and P. A. Johnson, "A set of measures for the systematic classification of the nonlinear elastic behavior of disparate rocks," *J Geophys Res-Sol Ea*, 120(3), 1587-1604, 2015.
- [15] K.W. Winkler and X. Liu, "Measurements of third order elastic constants in rocks." *J. Acoust Soc Am*, 133(6):3706 - 3718, 2013.